Effect of Solvation on Pinched Cone−Pinched Cone Interconversion of Tetraethoxycalix[4]arene and Tetraethoxythiacalix[4]arene

Jiří Matoušek,[†] Petr Kulhánek,[†,‡] Michal Čajan,[†,§] and Jaroslav Koča*[,†,‡]

National Centre for Biomolecular Research, Faculty of Science, Masaryk University in Brno, Kotlářská 2, CZ-611 37 Brno, Czech Republic, Department of Organic Chemistry, Faculty of Science, Masaryk University in Brno, Kotlářská 2, CZ-611 37 Brno, Czech Republic, and Laboratory of Growth Regulators, Palacký University and Institute of Experimental Botany AS CR, Šlechtitelů 11, CZ-783 71 Olomouc, Czech Republic

Received: September 23, 2005; In Final Form: November 23, 2005

The pinched cone−pinched cone interconversion (PCI) of tetraethoxy substituted calix[4]arene and thiacalix-[4]arene was studied by means of molecular dynamics using the GAFF force field and quantum mechanics. Influence of solvent was expressed by changes in cavity geometries as well as in free energy barriers that were calculated using constrained MD simulations. Water and chloroform were found to reduce the energy barriers in comparison with vacuum simulations. Only qualitative agreement between energy barriers calculated by MD and experimental values was achieved. Also, quantum chemical calculations were performed with the RI-MP2 method, and a better description of PCI was achieved than that previously obtained by HF or DFT methods. The combination of qualitative MD data on solvated systems with RI-MP2 gas-phase data gave us very good agreement with experimental results.

Introduction

Calix[4]arenes, the most popular building blocks in the field of supramolecular chemistry, can exist in four more or less stable conformations designated the *cone*, the *partial cone*, the *1,2-alternate*, and the *1,3-alternate* (Figure 1). It is well documented that the introduction of bulky substituents to the lower rim (phenolic hydroxyls) of calix[4]arene derivatives can lead to the immobilization of conformational movement and to the stabilization of these basic conformations. Any of these conformations represents a special three-dimensional arrangement with different complexation behavior and hence, with different potential applications as a molecular scaffold and advantageously useful building blocks in supramolecular chemistry.[1−4] On the other hand, experimental observations have indicated that these stabilized conformations are not absolutely rigid. This specific flexibility of the calixarene ring is closely related to its ability to interact with other molecules or ions, and also with its complexation properties and chemical reactivity.

Pinched cone−pinched cone interconversion (PCI) of the conic conformer is one example of slight conformational flexibility. The C_{4v} symmetry of the calixarene ring, observed usually in the ^{1}H NMR spectra, is in fact a time-averaged signal of two relatively stable conformations possessing lower C_{2v} symmetry. Thus, the structure with C_{4v} symmetry represents rather a transition state of the above-mentioned interconversion, while both C_{2v} conformers are the minima on the potential energy hypersurface (PES) (Figure 2). Several authors have studied this equilibrium in normal calix[4]arene series using dynamic ^{1}H NMR techniques.[5−9] As we reported recently,[10] the introduction of four sulfur atoms into the calixarene skeleton leads to a dramatic change in properties of the skeleton. Simple tetraalkylated derivatives of thiacalix[4]arene[11] possess interesting differences from the normal methylene bridged calix[4]arene derivatives,[12] among others in their conformational behavior. As we have found, the cone conformers of tetraalkylated thiacalix[4]arenes surprisingly demonstrate line broadening of their ^{1}H NMR spectra at room temperature while the coalescence phenomenon of normal tetraalkylated calix[4]arene derivatives was not observed even at the lowest temperatures accessible in the NMR experiments. Obviously, this reflects the great difference between the energy barriers of the studied process for both calixarenes.[10]

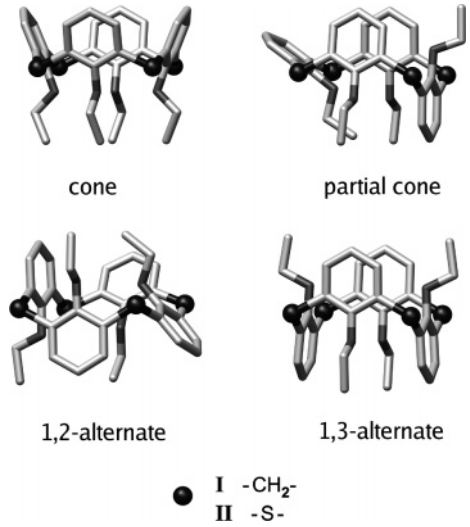

Figure 1. Basic conformations of calix[4]arene derivatives.

In this work, we compare the conformational properties of tetraethoxy[4]calixarene **I** and its thia-analogue **II** by means of molecular mechanics and dynamics (MD) and quantum mechanics (QM). Concerning the energy profile of the transition,

* Corresponding author. E-mail: jkoca@chemi.muni.cz.
† National Centre for Biomolecular Research, Faculty of Science, Masaryk University in Brno.
‡ Department of Organic Chemistry, Faculty of Science, Masaryk University in Brno.
§ Palacký University and Institute of Experimental Botany AS CR.

10.1021/jp055415r CCC: $33.50
Published on Web 12/24/2005

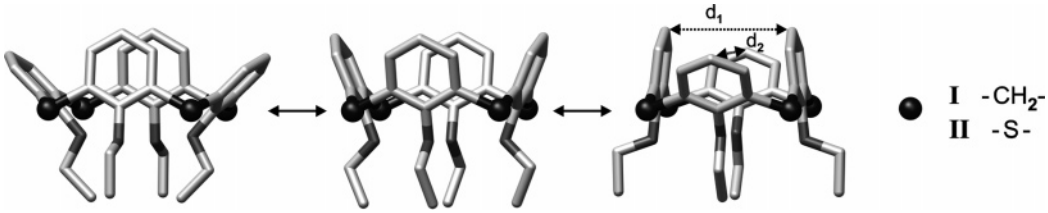

Figure 2. Graphic representation of pinched cone−pinched cone interconversion.

free energy activation barriers were calculated by the *potential of mean force* (PMF) approach based on MD simulations. The simulations were performed in three environments: vacuum, chloroform, and water. Special attention was devoted to the role of solvent molecules in the stabilization of stationary points found on the *free energy surface* (FES). Performed MD simulations as well as comparative QM studies indicate substantial differences between conformational properties of the normal and thiacalixarene cavities. The data obtained were compared with that from the NMR experiments.

Computational Details

Molecular Dynamics Simulations. Each calix[4]arene derivative was simulated in three different environments: vacuum (**v**), explicit chloroform (**c**), and explicit water (**w**). Each simulation is labeled according to the type of calixarene and the type of environment. For example, **Iv** refers to simulation of the calixarene **I** in a vacuum, and so on.

Vacuum simulations were performed with the SANDER module of the AMBER 7.0 package.[13] A molecule of corresponding calix[4]arene was energy minimized and then progressively heated from 5 to 298.15 K during the first 100 ps. Initial atom velocities at 5 K were assigned randomly according to a Boltzmann distribution. Rotational and translation movements were removed each 1 ps to prevent the system from becoming a flying cube-of-ice. After the system had been heated, data were collected from a 20 ns long simulation. Nonbonded interactions were calculated without any approximation. A constant temperature of 298.15 K was maintained by the weak coupling algorithm with a coupling constant of 1 ps. Translation and rotational movements were removed every 5 ps.

Simulations in explicit solvent were performed with the PMEMD module of the AMBER package. This module provides higher computational performance than the traditional SANDER module. System equilibration and production dynamics simulations were performed under similar conditions as in the case of vacuum simulations. The pressure of the system was maintained at 1 bar by the weak coupling algorithm with isotropic position scaling and with a relaxation time of 1.2 ps during the heating as well as during the production stage. Nonbonded interactions were approximated with the *particle-mesh Ewald method* (PME)[14] with direct summation truncated at 9 Å cutoff. Rectangular boxes with approximately the same 50 Å edge lengths were used in both solvents.

In all simulations, the integration step was 2 fs and the lengths of all bonds involving a hydrogen atom were constrained with the SHAKE algorithm. The force field parameters of calix[4]-arenes were taken from the *general Amber force field* (GAFF).[15] The RESP charges were calculated from the electrostatic potential by the ANTECHAMBER module of the AMBER package. Electrostatic potential was calculated by the HF/6-31G* quantum-chemical method on the geometry obtained by optimization of the corresponding calix[4]arene with the same method using the GAUSSIAN 98 package.[16] Parameters for water and chloroform molecules were taken from the TIP3P model and the CHCL3BOX model, respectively. These parameters are distributed within the AMBER package.

Free Energy Calculations. Modified versions of the SANDER and PMEMD programs from the AMBER package were used to perform *potential of mean force* (PMF) calculations. The distance d_1 between adjacent carbon atoms in the upper rim was used as the coordinate that drives the change from one pinched cone conformer to the other one (Figure 2). There are at least four methods that can be used to calculate PMF in our case: *weighted histogram techniques*,[17,18] *Jarzynski's identity based method*,[19] *the constraint dynamics approach*,[20,21] and *the adaptive biasing force aproach*.[22] For our purposes, a multidimensional version of the constraint dynamics approach was used.[22,23,24] Free energy is not obtained directly by the method. Instead, its first derivative is calculated along the pathway by the following formula 1

$$\frac{\partial W}{\partial \xi'_\alpha} = \frac{\langle |\Xi|^{-1/2}[(k_B T/2)G_\alpha - \lambda_\alpha]\rangle_{\xi'}}{\langle |\Xi|^{-1/2}\rangle_{\xi'}} \qquad (1)$$

where k_B is the Boltzmann constant, T is the temperature, Ξ is the weight matrix, G_α is the correction factor, and λ_α is the Lagrange multiplier of the constraint. Possible coupling between the driven distance d_1 and other constraints (bonds constrained by SHAKE) in the system was neglected even though the way to solve this situation is known.[25] Our practical experience shows that this coupling is negligible for the studied system.

Sixty-five (calixarene **I**) and seventy-five (calixarene **II**) simulations (windows) with increasing values of the driven distance d_1 were used for construction of the free energy profile. Each window consists of a 50 ps equilibration and a 500 ps accumulation stage. MD simulations consisting of two repeating steps were used to prepare starting structures for the individual windows. In the first step, the driven distance was elongated by about 0.1 Å in 20 ps, and in the second step, the system was equilibrated during 50 ps. Final coordinates and velocities from the end of the second step were used as a starting point for the particular window simulation. Free energy profiles of PCI were calculated in three environments with the same simulation conditions as mentioned in the *Molecular Dynamics Simulations* section.

Analysis of Solvent Interaction with the Calixarene Cavity. Solvent analysis was performed on 5 ns long simulations, in which the driven distance d_1 was constrained on values corresponding to stationary states. The simulation conditions were the same as mentioned before. Analysis was based on the calculation of density maps, which show the occurrence of each solvent atom in the given space. If a solvent molecule specifically interacts with the solute, a higher density in interaction space is exhibited. The maps were calculated by the PTRAJ module of the AMBER package. Raw maps were smoothed by the *fast Fourier transform* (FFT) technique with an included low-pass filter, the threshold of which was set to 20%. The final maps were visualized and analyzed using the CHIMERA program.[26]

TABLE 1: Summary of Molecular Dynamics Simulation Results[a]

		MD			PMF					
		d_1	d_2	Δd_{2-1}	d_1(**S1**)	d_1(**S2**)	Δd_{S2-S1}	d_1(**TS**)	ΔG_1	ΔG_2
I	vacuum	5.01	9.84	4.83	5.0	9.9	4.9	7.8	3.85	0.08
	chloroform	5.48	9.72	4.24	5.4	9.7	4.3	7.9	0.85	0.17
	water	6.27	9.21	2.94	6.3	9.2	2.9	7.9	2.26	−0.05
II	vacuum	4.38	10.05	5.67	4.4	10.0	5.6	7.8	5.81	−0.06
	chloroform	4.38	10.05	5.67	4.3	10.0	5.7	7.8	2.90	0.13
	water	4.38	10.05	5.67	4.1	10.0	5.9	7.7	3.61	−0.09

[a] Δd_{2-1} is cavity deformability from MD simulations; d_1(S1), d_1(S2), and d_1(TS) represent values of driven distance in stationary states from PMF calculations; S1, first minimum, S2, second minimum, TS, transition state; Δd_{S2-s1} is cavity deformability from PMF; ΔG_1 is the activation barrier of PCI; ΔG_2 is the energy difference between S1 and S2 (distances in Å, energies in kcal/mol). Values of d_1 and d_2 for structures with the highest occurrence in histogram analysis.

Quantum Mechanical Calculations. Activation barriers of pinched cone−pinched cone interconversion were also calculated with the RI-MP2 method implemented in the TURBOMOLE 5.6 program.[27] The RI-MP2 approach differs from the standard MP2 perturbation method in the treatment of coulomb integrals. These integrals are calculated with projected wave function on a smaller specially optimized basis set, which speeds up the calculation enormously while introducing low level of error.[28] For each calix[4]arene, two calculations of activation energies were carried out with the cc-pVDZ and aug-cc-pVDZ basis sets. Since it is still very computationally demanding to carry out optimization with the RI-MP2 method, geometries obtained with the B3LYP hybrid functional and 6-31G** basis were used.[10]

Results and Discussion

Molecular Dynamics. Molecular dynamics simulations were used to describe the properties and conformational behavior of two types of calixarenes, **I** and **II**. The flexibility of the calixarene cavity was first expressed by the time-dependent change of the distances d_1 and d_2 between carbon atoms in the *para* positions of two opposite aromatic rings. This information is necessary for proper setup of the PMF calculations as well as its ability to provide a preliminary insight into the role of solvent effects in the PCI process. Selected distances were thoroughly analyzed by histogram analysis (Figure 3). Analysis was carried out in a range from 3.0 to 11.0 Å and with a bin width of 0.21 Å. Positions of bin centers are used in further discussion about geometrical considerations.

The values of distances d_1 and d_2 for states with the highest occurrences (two pinched cone conformers) are summarized in Table 1. These values can be used to calculate cavity deformation expressed as the absolute value of the difference between them. A lower value of the given quantity thus means that the cavity is more symmetrical than when in the opposite situation. In the case of calixarene **I**, the values of cavity deformation are 4.83, 4.24, and 2.94 Å for simulations in a vacuum, chloroform, and water environments, respectively. The cavity deformation of calixarene **II** is 5.67 Å and it does not depend on the environments used. The larger cavity deformation observed for calixarene **II** can be explained by the presence of bridging sulfur atoms. The C_{ar}−S bond is longer by about 0.2 Å compared to the corresponding C_{ar}−C bond in calixarene **I**. The longer C_{ar}−S bond is thus responsible for the large deformation of the calixarene **II** cavity. The wide variation of cavity deformation for calixarene **I** shows its higher flexibility compared to calixarene **II**. Surprisingly, the smallest deformation was observed for the simulation of calixarene **I** in water. This will be discussed in more details in the section related to the cavity interactions with solvent.

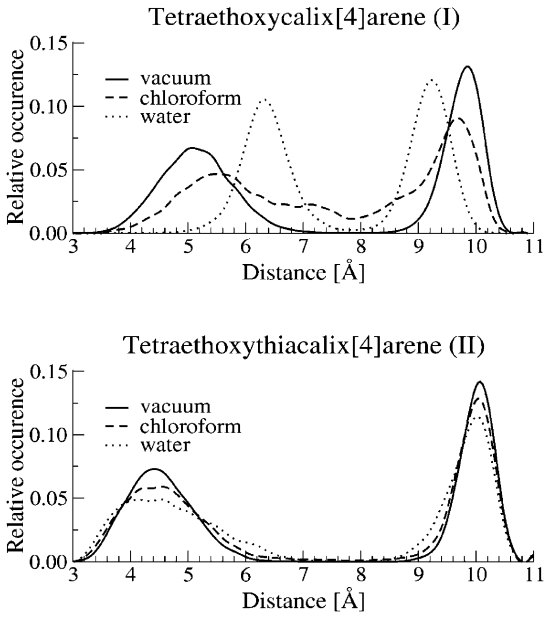

Figure 3. Histogram analysis of selected distances d_1 and d_2 in three different environments for calixarene **I** (top) and **II** (bottom), bin width is 0.21 Å.

The results from the MD simulations allow for qualitative conclusions about the activation energies of PCI. It is immediately clear that the energy barrier of PCI of calixarene **I** in chloroform is the lowest from all studied situations. This is judged on the basis of the highest occurrence of intermediate states during the course of PCI. Energy barriers for other simulations cannot be so easily estimated because their intermediate states are not sufficiently sampled. In this situation, the number of PCIs that occur during the 20 ns long simulation is used for such estimations. The only case in which PCI was not observed to occur was in the simulation of calixarene **II** in a vacuum. This indicates that the energy barrier of such PCI should be higher than that of the other systems. Three simulations **Iv**, **IIw**, and **IIc** revealed approximately the same occurrence of PCI (from 3 to 4). A 10-times-higher occurrence of PCI was found for the simulation of calixarene **I** in water; thus, such PCI has to be less energetically demanding. The calculation of PCI events was not possible for **Ic** simulation because of high occurrence of states that are very close to a transition state (see Figure 4). In the next section, quantitative values of activation barriers calculated by the PMF approach will be presented and discussed.

Potential of Mean Force Calculations. The results of all PMF calculations are shown in Figure 4. Calculated PMF curves show two minima separated by a barrier. The minima correspond to two equivalent pinched-cone conformers. Their calculated energies, which have to be the same, are slightly different in

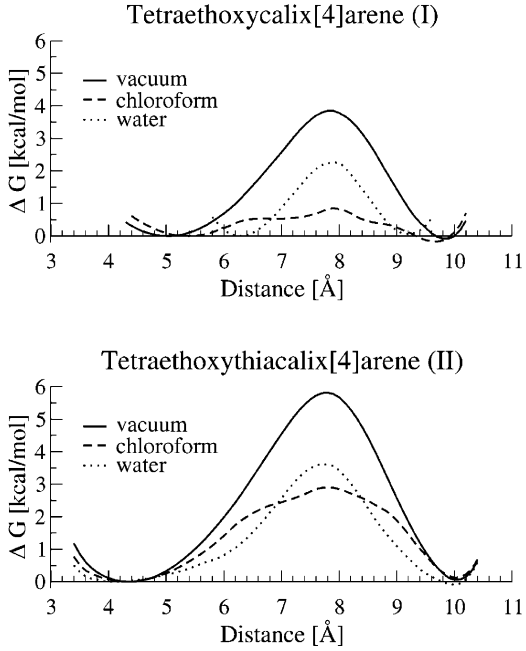

Figure 4. Comparison of free energy profiles of PCI in three different environments for calixarene **I** (top) and **II** (bottom).

our calculations. Errors result from the numerical calculations of the first derivative of the free energy and from its numerical integration leading to the final free energy profile. Introduced errors can be analyzed via several approaches, which are generally rather complicated. However, a very simple approach can be used in our case. Since both minima have to have the same energy, the introduced errors are simply equal to the differences between the calculated energies of the two minima. The absolute values of such differences are lower than 0.17 kcal/mol for six independent calculations. The errors in energy barriers should be even lower because the number of points used in numerical integration is lower than that for the integration from one minimum to the other one. Of course, it must be remembered that there are other sources of errors that are connected to the force field parameters used, MD methodology, etc.

The results extracted from PMF curves are summarized in Table 1. The energy barriers for simulation in a vacuum are 3.85 and 5.81 kcal/mol for calixarene **I** and **II**, respectively. The presence of solvent molecules leads to the reduction of the energy barriers. Chloroform reduces them by about 3 kcal/mol regardless of calixarene type. In contrast, the reductions in the height of the energy barriers in water environment slightly depend on calixarene type. A reduction of 1.6 kcal/mol was found for calixarene **I** and 2.2 kcal/mol for calixarene **II**. The energy barriers in chloroform have been greatly underestimated when they were compared with the ones derived from the experiments.[10] The differences are 7.65 (upper estimate) and 9.00 kcal/mol for calixarene **I** and **II**, respectively. This shows that the GAFF force field is not able to predict correct values of energy barriers. However, it is important that the qualitative order is predicted correctly. It means that the PCI of calixarene **II** is slower than that of calixarene **I**. Possible reasons for such a high inconsistency between experimental and calculated values will be discussed in more detail in the *Quantum Chemical Calculations* section.

Analysis of Interactions between Solvent and Calixarenes. Previous analysis of MD simulations and PMF calculations shows a significant influence of solvent on PCI. It has been found that the solvent generally reduces the energy barriers of PCI. In the case of calixarene **I**, it even influences the geometry of pinched cone conformers. To explain this behavior in more detail, a detailed analysis of interactions between the solvent and the calixarene skeleton was carried out. For this purpose, additional simulations of 5 ns length were run with an imposed constraint on d_1 distance. The length of the constrained distance was chosen according to estimated stationary points of the free energy profiles to represent either the pinched cone conformer (**S1**) or the transition state (**TS**) of PCI.

Interactions between the solvent and the calixarenes were analyzed according to the densities of each solvent atom type in the close neighborhood of the calixarene molecule. The basic idea of this approach is that a stronger interaction between the solvent and the calixarene molecules should result in the longer stay and hence in the higher occurrence (density) of the solvent molecule in the given space element. As this approach can be used for each atom type of the solvent molecule, it could also be employed to show the preferred orientation of the solvent molecule in the interaction site. However, changes in solvent density are relatively small and the identification of interaction sites is complicated. Therefore, the obtained densities were processed by *fast Fourier transform* to remove noise and to highlight places with higher densities. Density maps processed by this approach show time averaged situations and they can therefore represent a superposition of several molecules. The final density maps for both studied types of calixarene are shown in Figures 5 and 6.

Density analysis of chloroform interactions with **S1** of calixarene **I** shows six interaction sites. Two of them represent molecules interacting with the inner part of the cavity via the upper rim and they correspond to one or two solvent molecules. Each of them is oriented by the C−H bond to the aromatic ring, and the chlorine atoms are then pointed away from the cavity. The remaining four interaction sites are outside the cavity. Two of them are well shaped and they show the same orientation of the C−H bond to the aromatic ring. The last two sites show the presence of chloroform molecules close to the aromatic rings without information about the molecule's orientations. The reason for this is that these rings are not constrained and therefore, due to their larger fluctuations, the densities of hydrogen and chlorine atoms are not well enough defined to show significant values in these regions. The situation for calixarene **II** is different. Only two sites are observable in the density map. They represent one or two solvent molecules that are located above the more distant aromatic rings. In contrast to calixarene **I**, the chlorine atoms point toward the cavity and the hydrogen atoms away from it.

In the transition states (**TS**) of both calixarene **I** and **II**, the density maps show only one significant interaction site, which is situated within the cavity. The observed densities represent the superposition of several orientations of one molecule. One chlorine atom of this molecule is deeply engaged in the cavity, which is a common feature for both calixarenes. However, the calixarenes differ in the preferred orientations of the C−H bond. The bond points either to the aromatic rings or to methylene bridges in the case of calixarene **I**, but only to sulfur bridges in the case of calixarene **II**.

Density maps of water molecules show a different structure of interaction sites than that for chloroform. For the **S1** structure of calixarene **I**, seven interaction sites were found. Three of them are grouped in a small cluster within the cavity. One water molecule forms a bridge between the closer aromatic rings, and the hydrogens of this molecule point to these rings. The other two water molecules are bonded to the oxygen of the bridge

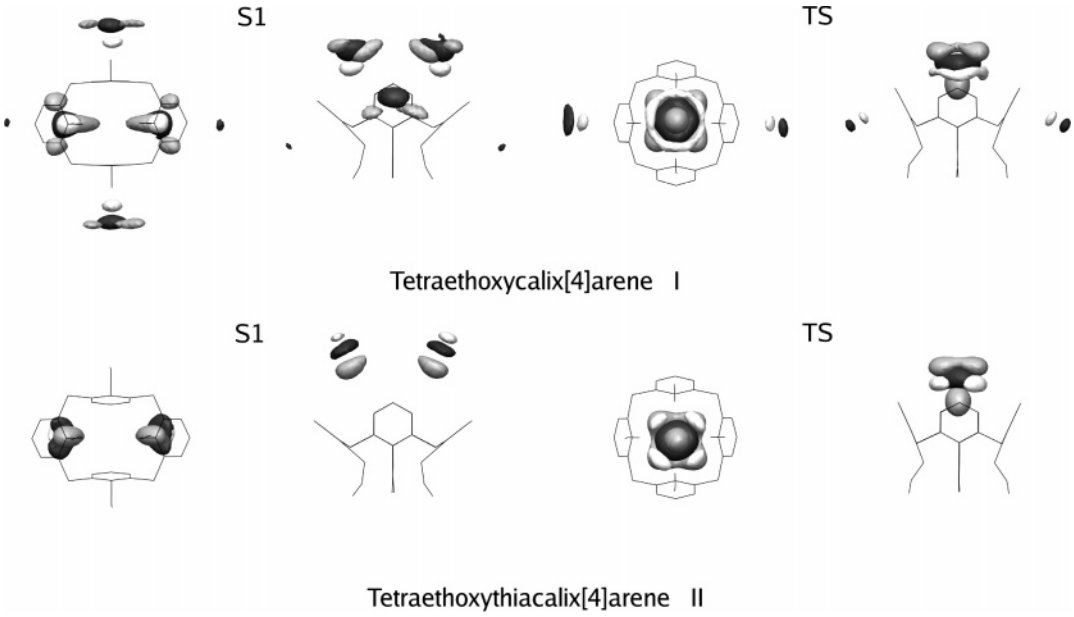

Figure 5. Interaction with chloroform. Bottom and side views for **S1** and **TS** structures: gray, chlorine; dark gray, carbon; white, hydrogen. (Color version is given in the Supporting Information as Figure 1S.)

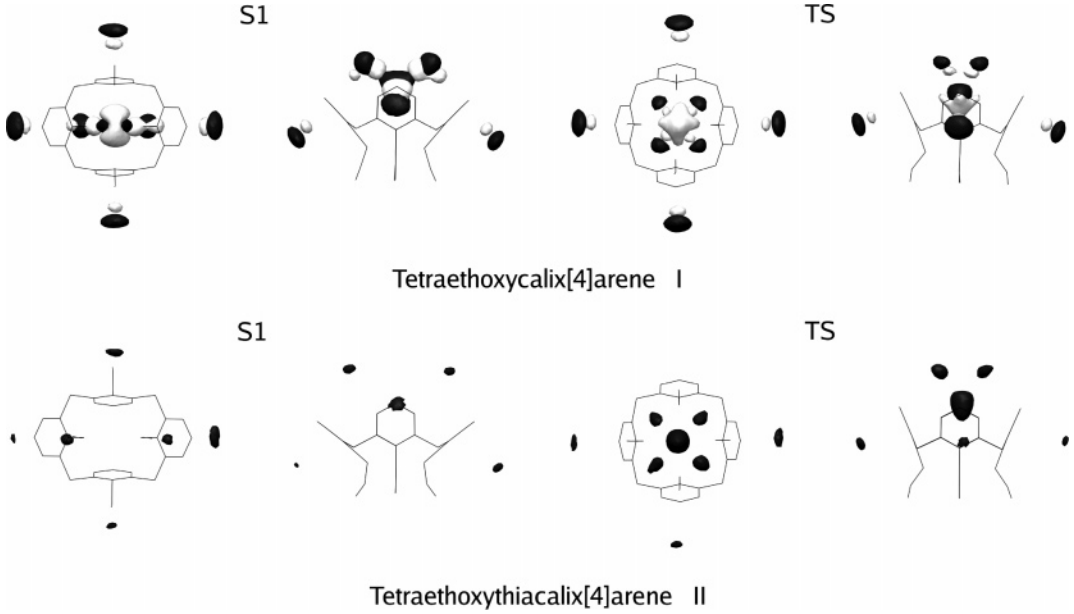

Figure 6. Interaction with water. Bottom and side views for **S1** and **TS** structures: black, oxygen; white, hydrogen. (Color version is given in the Supporting Information as Figure 2S.)

water molecule by hydrogen bonds. Their second hydrogens point to the remaining aromatic rings. This complex type was observed experimentally in similar calixarene derivative.[29] The other interaction sites are situated outside the cavity close to the aromatic rings. In the case of calixarene **II**, no significant interaction sites were found either inside or outside the cavity.

In the transition state (**TS**) of calixarene **I**, four sites around the cavity and a cluster of several water molecules within the cavity were observed. The core of the cluster is formed by one water molecule situated deeply within the cavity. Its hydrogen atoms are oriented either to the aromatic rings or to the center of the cavity. Four other sites are located above this water molecule. However, detailed analysis shows the coexistence of two molecules in these positions. Consequently, a superposition of them is seen in the density map. A similar cluster is formed also in the **TS** of calixarene **II**, but the orientation of the water molecules cannot be determined in this case because the hydrogen density map does not exhibit any meaningful regions with higher values.

Examples of some complexes formed between solvent and calixarenes **I** and **II** are shown in Figures 3S, 4S, and 5S in the Supporting Information.

The above analysis shows that the cavity interacts specifically with the solvent in all transition states (**TS**). The interaction is mostly caused by the presence of a single solvent molecule within the cavity. On the other hand, interaction sites in pinched cone conformers (**S1**) are well established only in the case of calixarene **I**. The presence of a solvent molecule inside the cavity of the TS could explain the observed reduction in the free energy barrier of PCI in the solvent. The interesting water cluster formed inside the cavity in structure **S1** of calixarene **I** is also responsible for the significantly different behavior of this compound in water environment during the molecular dynamics

TABLE 2: Experimental Free Energy Barrier (ΔG_{Exp}) and Calculated Electronic Energy Barriers (ΔE) of PCI for Calixarene I and II (all in kcal/mol)

	6-31G**[a]		cc-pVDZ		aug-cc-pVDZ		
	ΔE(HF)	ΔE(B3LYP)	ΔE(HF)	ΔE(RI-MP2)	ΔE(HF)	ΔE(RI-MP2)	ΔG_{exp}[a]
I	6.48	5.76	6.54	8.66	6.42	9.51	<8.5
II	6.34	7.13	6.18	12.55	6.32	15.09	11.9

[a] Data taken from our previous work; for details see ref 10.

simulations compared to the simulations in the other environments.

Quantum Chemical Calculations. Our previous results based on HF and DFT calculations[10] provided relatively similar values of activation energies for the PCI process for both calixarenes **I** and **II**. On the other hand, experimentally obtained data[10] show a difference of about 4 kcal/mol between the activation barriers. Furthermore, the calculated barriers are underestimated by 2 kcal/mol (calixarene **I**) and 5 kcal/mol (calixarene **II**) compared to the corresponding experimental values. This discrepancy cannot be explained only as being due to solvent effects that were omitted in our previous calculations. As we have shown in previous sections, the solvent reduces energy barriers by approximately 3 kcal/mol (vacuum → chloroform) regardless of the calixarene type. This then means that QM calculations should lead to higher energy barriers than those measured experimentally.

A possible explanation for the failure of HF and DFT calculations could be that there was incorrect evaluation of dispersion interaction between the aromatic rings. Four aromatic rings are close enough to allow the significant interaction of their pi-electrons. The different geometries of pinched cone minima and PCI transition states as well as the different electronic character of calixarene bridges could then lead to the differing intensity of these interactions, and to the differing total energies of these molecules. Therefore, we have decided to recalculate the PCI barriers with more precise methods. As the best candidate, the RI-MP2 method was chosen, which provides a better description of dispersion interactions than previously used methods. In consistency with former calculations,[10] structures with C_{2v} symmetry for **I** and C_s symmetry for **II** were used as representatives of pinched cone conformers. Similarly, structures with C_4 symmetry were used as the transition states of PCI. The RI-MP2 corrections to HF energy barriers obtained with the cc-pVDZ basis were 2.12 and 6.37 kcal/mol for calixarene **I** and **II**, respectively. Thus, the final energy barriers were 8.66 and 12.55 kcal/mol, respectively. These values are in good agreement with the experimental observations and properly show the difference between the rates of PCI movement. When the aug-cc-pVDZ basis was used, final energy barriers were 9.51 and 15.09 kcal/mol for calixarene **I** and **II**, respectively. These barriers are higher than the experimental ones. Such overestimation is in consistency with the presented PMF calculations, which predicted the reduction of energy barriers by the solvent. Considering this we may suggest the missing experimental value for calixarene **I** to be around 6.5 kcal/mol.

Conclusions

In the presented study, the pinched cone−pinched cone conformational interconversion of tetraethoxycalix[4]arene **I** and tetraethoxythiacalix[4]arene **II** was studied by means of molecular dynamics and quantum mechanics. Molecular dynamics studies including the *potential of mean force* free energy calculations gave an interesting insight into the role of the solvent in the studied interconversions. A reduction in free energy barriers was observed in the presence of the solvent in comparison with simulations in a vacuum. This was about 3 kcal/mol for both calixarenes in chloroform. The influence of water on the energy barriers was less significant and lead to a reduction of only 1.6 and 2.2 kcal/mol for **I** and **II**, respectively. The presence of the solvent has an impact also on the geometry of the calixarene cavity. The largest changes were observed in the case of calixarene **I**, especially in its simulation with water. In this particular case, the cavity deformation in pinched cone conformer was about 2.9 Å whereas values within the range of between 4 and 5 Å were found in the remaining simulations of calixarene **I**. In the case of calixarene **II**, the observed deformation was about 5.7 Å in all environments used.

It follows from the detailed solvent analysis that the inner part of the calixarene cavity is the most important interaction site for solvent molecules. This could explain the observed reductions in energy barriers in the solvent. Analyses also showed the formation of small water clusters in structure **S1** of calixarene **I**, which could be responsible for the observed small cavity deformation.

The obtained molecular dynamics results show good qualitative agreement with experimental data. Concerning the quantitative energy analysis, the *general Amber force field* strongly underestimates the absolute values of PCI free energy barriers. Consequently, quantum chemical calculations with the RI-MP2 method were performed. Energy barriers obtained with the aug-cc-pVDZ basis set are 9.5 and 15.1 kcal/mol for calixarene **I** and **II**, respectively. These values are overestimated in comparison with those obtained by NMR. However, these RI-MP2 data do not contain entropy and solvation contributions. Since the molecular dynamics studies show the significant role of the solvent in the stabilization of the PCI transition state, obtained RI-MP2 energy barriers are more reasonable than in previously calculated data.[10]

Acknowledgment. The authors thank the Supercomputing Centre in Brno, Czech Republic, for providing access to computer facilities. We would also like to thank Martin Petřek for help with density map processing via FFT filtering. Financial support from the Ministry of Education, Youth, and Physical Training of the Czech Republic (Contract No. MSM0021622413), from the Grant Agency of the Academy of Sciences of the Czech Republic (Grant No. IAA400200503), and from the Grant Agency of the Czech Republic (Grant No. 204/03/H016) is gratefully acknowledged.

Supporting Information Available: Color versions of Figures 5 and 6 are presented as Figure 1S and 2S, respectively. Selected snapshots from constrained molecular dynamics simulations showing structures of complexes between solvent and calixarenes are summarized in Figures 3S, 4S, and 5S. Figure 3S shows the complex between calixarene **I** and chloroform molecule. Figure 4S shows the complex between calixarene **I** and water molecules, and finally, Figure 5S shows the complex between calixarene **II** and chloroform molecule. This material is available free of charge via the Internet at http://pubs.acs.org.

References and Notes

(1) *Calixarenes 2001*; Asfari, Z., Böhmer, V., Harrowfield, J., Vicens, J., Eds.; Kluwer Academic Publishers: Dordrecht, The Netherlands, 2001.

(2) Gutsche, C. D. In *Calixarenes revisited*; Stoddart, J. F., Ed.; Monographs in Supramolecular Chemistry 6; The Royal Society of Chemistry: Cambridge, U.K., 1998; Vol. 6.

(3) *Calixarenes 50th Aniversary: Commemorative Issue*; Vicens, J., Asfari, Z., Harrowfield, J. M., Eds.; Kluver Academic Publishers: Dordrecht, The Netherlands, 1994.

(4) C*alixarenes: A Versatile Class of Macrocyclic Compounds*; Vicens, J., Böhmer, V., Eds.; Kluwer Academic Publishers: Dordrecht, The Netherlands, 1991.

(5) Thondorf, I.; Brenn, J.; Böhmer, V. *Tetrahedron* **1998**, *54*, 12823−12828.

(6) Harada, T.; Shinkai, S. *J. Chem. Soc., Perkin Trans. 2* **1995**, 2231−2242.

(7) Soi, A.; Bauer, W.; Mauser, H.; Moll, C.; Hampel, F.; Hirsch, A. *J. Chem. Soc., Perkin Trans. 2* **1998**, 1471−1478.

(8) Ikeda, A.; Tsuzuki, H.; Shinkai, S. *J. Chem. Soc., Perkin Trans. 2* **1994**, 2073−2080.

(9) Lang, J.; Vlach, J.; Dvořáková, H.; Lhoták, P.; Himl, M.; Hrabal, R.; Stibor, I. *J. Chem. Soc., Perkin Trans. 2* **2001**, 576−580.

(10) Čajan, M.; Lhoták, P.; Lang, J.; Dvořáková, H.; Stibor, I.; Koča, J. *J. Chem. Soc., Perkin Trans. 2* **2002**, 1922−1929.

(11) Lhoták, P.; Himl, M.; Pakhomova, S.; Stibor, I. *Tetrahedron Lett.* **1998**, *39*, 8915−8918.

(12) Lhoták, P. *Tetrahedron* **2001**, *57*, 4775−4779.

(13) Case, D. A.; Pearlman, D. A.; Caldwell, J. W.; Cheatham, T. E., III; Wang, J.; Ross, W. S.; Simmerling, C. L.; Daren, T. A.; Merz, K. M.; Staton, R. V.; Cheng, A. L.; Vincent, J. J.; Crowley, M.; Tsui, V.; Gohlke, H.; Radmer, R. J.; Duan, Y.; Pitera, J.; Massova, I.; Seibel, G. L.; Singh, U. C.; Weiner, P. K.; Kollman, P. A. *AMBER 7;* University of California: San Francisco, CA, 2002.

(14) Darden, T.; York, D.; Pedersen, L. *J. Chem. Phys.* **1993**, *98*, 10089−10092.

(15) Wang, J. M.; Wolf, R. M.; Caldwell, J. W.; Kollman, P. A.; Case, D. A. *J. Comput. Chem.* **2004**, *25*, 1157−1174.

(16) Frisch, M. J.; Trucks, G. W.; Schlegel, H. B.; Scuseria, G. E.; Robb, M. A.; Cheeseman, J. R.; Zakrzewski, V. G.; Montgomery, J. A., Jr.; Stratmann, R. E.; Burant, J. C.; Dapprich, S.; Millam, J. M.; Daniels, A. D.; Kudin, K. N.; Strain, M. C.; Farkas, O.; Tomasi, J.; Barone, V.; Cossi, M.; Cammi, R.; Mennucci, B.; Pomelli, C.; Adamo, C.; Clifford, S.; Ochterski, J.; Petersson, G. A.; Ayala, P. Y.; Cui, Q.; Morokuma, K.; Malick, D. K.; Rabuck, A. D.; Raghavachari, K.; Foresman, J. B.; Cioslowski, J.; Ortiz, J. V.; Baboul, A. G.; Stefanov, B. B.; Liu, G.; Liashenko, A.; Piskorz, P.; Komaromi, I.; Gomperts, R.; Martin, R. L.; Fox, D. J.; Keith, T.; Al-Laham, M. A.; Peng, C. Y.; Nanayakkara, A.; Gonzalez, C.; Challacombe, M.; Gill, P. M. W.; Johnson, B. G.; Chen, W.; Wong, M. W.; Andres, J. L.; Head-Gordon, M.; Replogle, E. S.; Pople, J. A. *Gaussian 98 (Revision A.9)*; Gaussian, Inc.: Pittsburgh, PA, 1998.

(17) Kumar, S.; Rosenberg, J. M.; Bouzida, D.; Swendsen, R. H.; Kollman, P. A. *J. Comput. Chem.* **1995**, *16*, 1339−1350.

(18) Roux, B. *Comput. Phys. Commun.* **1995**, *91*, 247−282.

(19) Jarzynski, C. *Phys. Rev. Lett.* **1997**, *78*, 2690−2693.

(20) Sprik, M.; Ciccotti, G. *J. Chem. Phys.* **1998**, *109*, 7737−7744.

(21) den Otter, W. K.; Briels, W. J. *J. Chem. Phys.* **1998**, *109*, 4139−4146.

(22) Darve, E.; Pohorille, A. *J. Chem. Phys.* **2001**, *115*, 9169−9183.

(23) den Otter, W. K.; Briels, W. J. *Mol. Phys.* **2000**, *98*, 773−781.

(24) Sergi, A.; Ciccotti, G.; Falconi, M.; Desideri, A.; Ferrario, M. *J. Chem. Phys.* **2002**, *116*, 6329−6338.

(25) Coluzza, I.; Sprik, M.; Ciccotti, G. *Mol. Phys.* **2003**, *101*, 2885−2894.

(26) Pettersen, E. F.; Goddard, T. D.; Huang, C. C.; Couch, G. S.; Greenblatt, D. M.; Meng, E. C.; Ferrin, T. E. *J. Comput. Chem.* **2004**, *25*, 1605−1612.

(27) Eichkorn, K.; Treutler, O.; Öhm, H.; Häser, M.; Ahlrichs, R. *Chem. Phys. Lett.* **1995**, *242*, 652−660.

(28) Jurečka, P.; Nachtigall, P.; Hobza, P. *Phys. Chem. Chem. Phys.* **2001**, *3*, 4578−4582.

(29) Atwood, J. L.; Harnada, F.; Robinson, K. D.; Orr, G. W.; Vincent, R. L. *Nature* **1991**, *349*, 683−684.